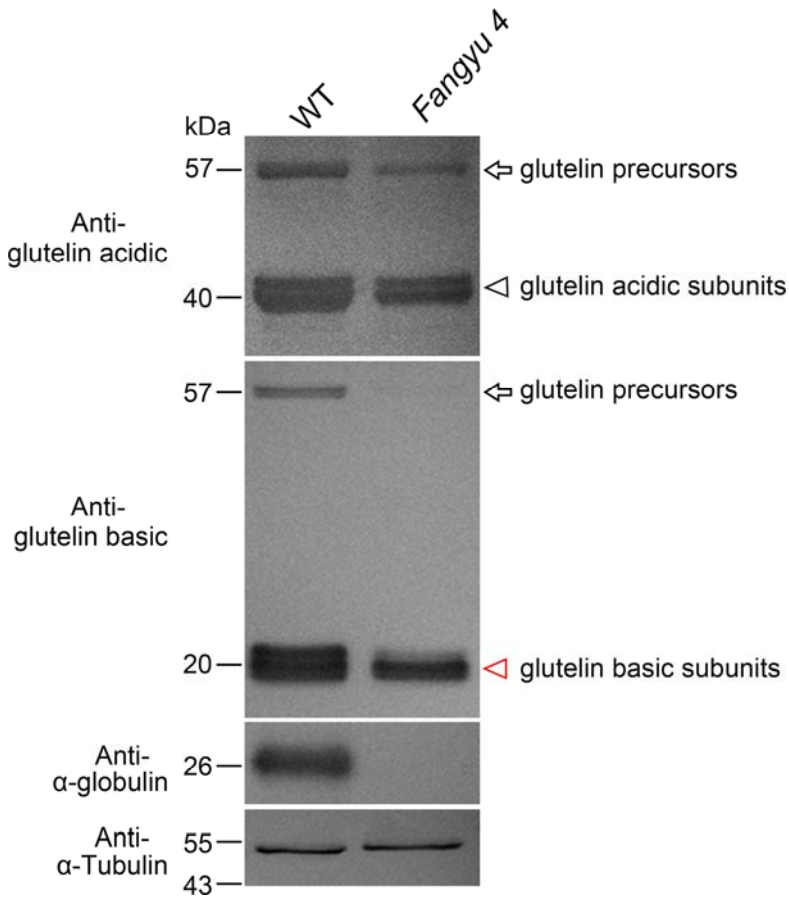

Supplemental Figure 1. Evaluation of the specificity of the storage protein monoclonal antibodies developed in this work.
Immunoblot assay showing that both antibodies against the glutelin acidic and basic subunits can react strongly with proglutelins and their respective subunits in wild type (WT), but weaker interaction in *Fangyu4* (a low glutelins *japonica* var). In contrast, the anti-α-globulin antibodies recognize a specific band in WT but not in *Fangyu4* (a 26-kD α-globulin deficient *japonica* var). These data confirmed that the antibodies are specific for the glutelin acidic subunits, basic subunits, and α-globulins, respectively. Arrows denote the 57-kD proglutelins, while arrowheads indicate the glutelin acidic subunits (black) and basic subunits (red), respectively. Anti-α-Tubulin antibodies were used as a loading control.

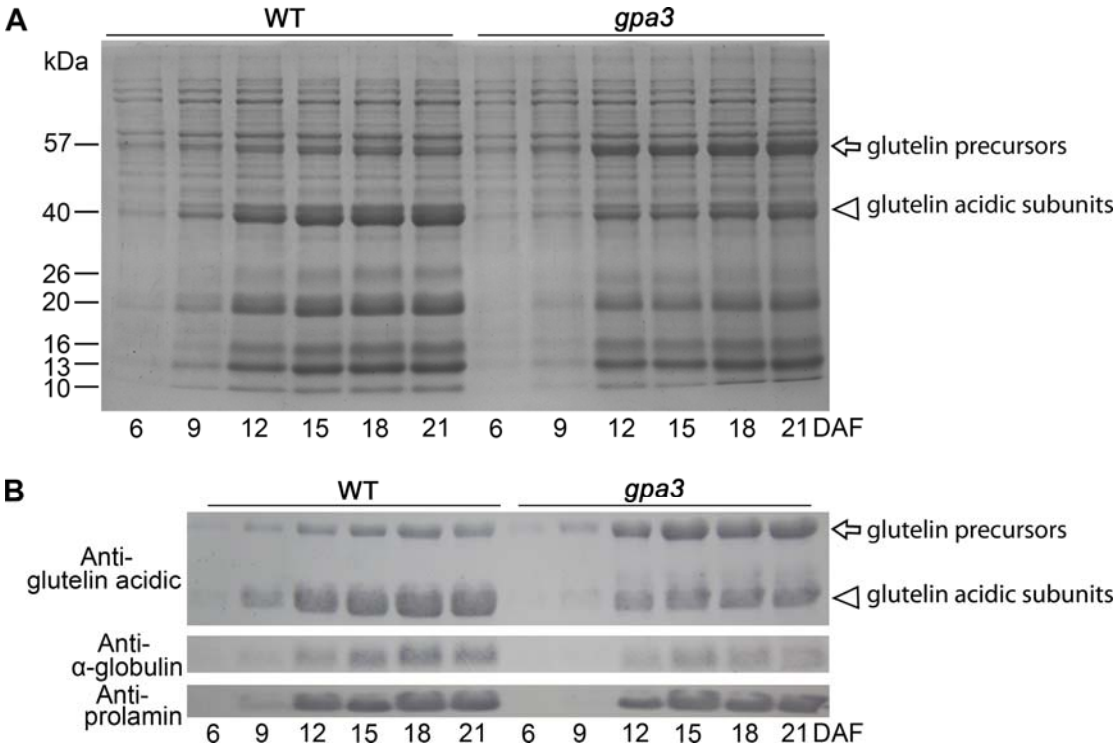

Supplemental Figure 2. Time course analysis of storage proteins during wild-type and *gpa3* endosperm development.

(A) SDS-PAGE analyses of seed storage proteins during wild type (WT) and *gpa3* endosperm development. Increased accumulation of glutelin precursors (arrows) and reduced accumulation of the acidic subunits (arrowhead) become visible in 9 DAF endosperm and obvious in 12 DAF endosperm and thereafter. DAF, days after flowering.

(B) Immunoblot analysis showing altered accumulation of glutelins, α-globulins, and 13-kD prolamins in *gpa3* endosperm development. DAF, days after flowering.

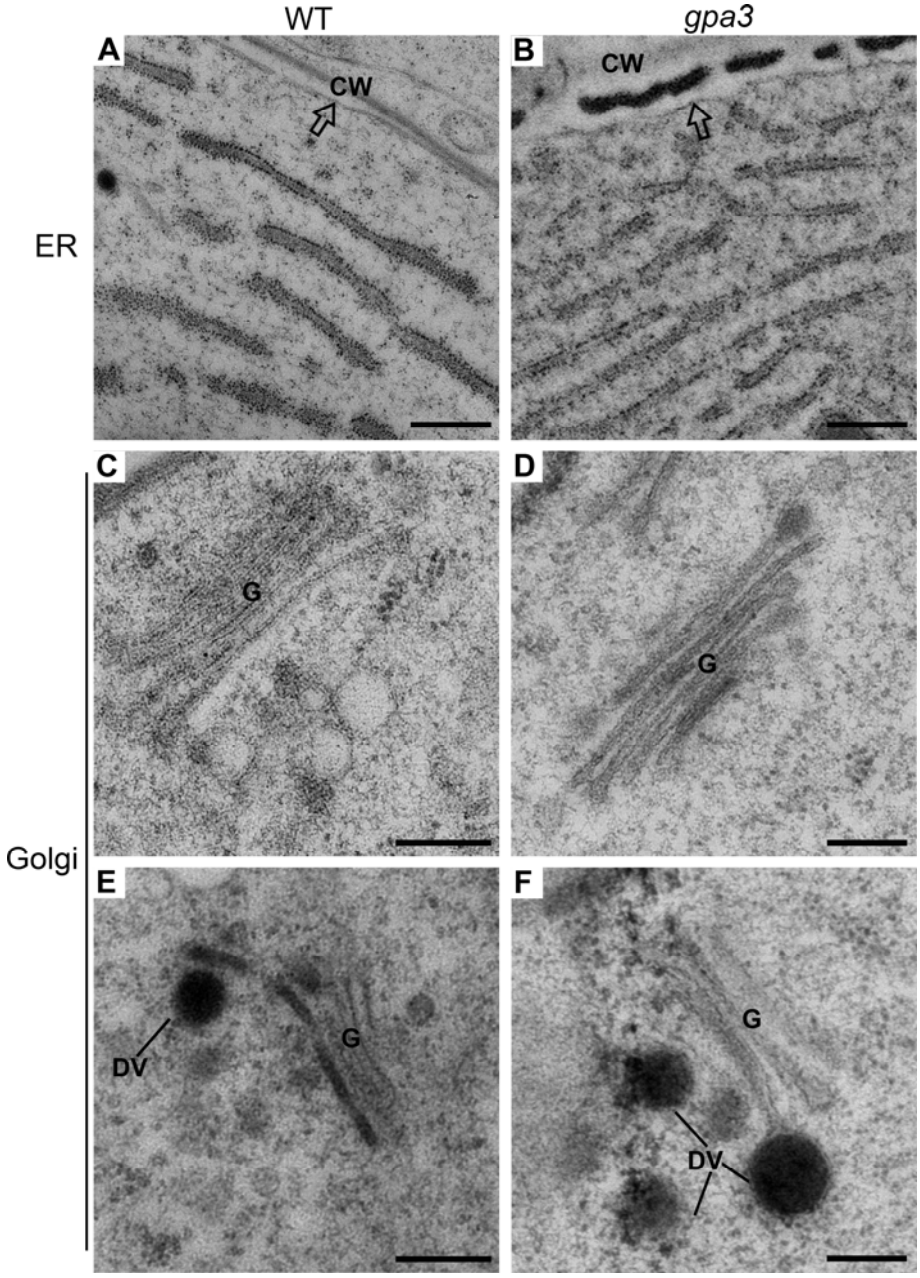

Supplemental Figure 3. The morphology of ER and Golgi in developing wild-type and *gpa3* subaleurone cells.

Developing wild-type and *gpa3* endosperm (9 DAF) were collected, and the peripheral region containing the subaleurone cell layers were subject to high-pressure frozen/freeze substitution (HPF) treatment, and then embeded in HM20. Ultrathin sections were then prepared, and examined using transmission electron microscope (TEM). No obvious defects in ER and Golgi were detected in *gpa3* in comparison with those of wild type. Arrows indicate the plasma membrane. ER, the endoplasmic reticulum; CW, cell wall; G, the Golgi apparatus; DV, dense vesicle. DAF, days after flowering. Bars in **(A)** and **(B)** = 500 nm; bars in **(C)** to **(F)** = 200 nm.

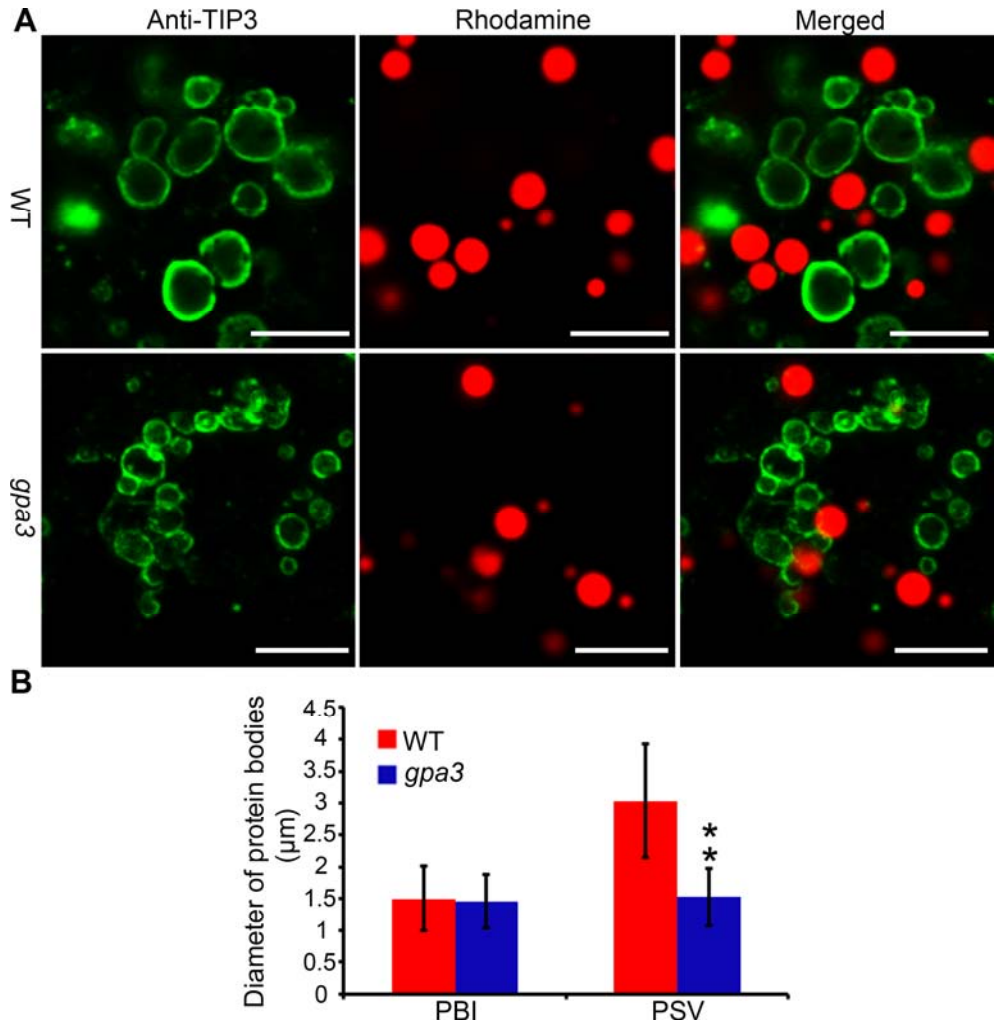

Supplemental Figure 4. *gpa3* forms smaller PSVs in comparison with the wild type.

(A) Confocal microscopy images of TIP3-marked protein storage vacuoles (PSVs, green) and Rhodamine-labeled PBIs (red) in wild-type (WT) and *gpa3* subaleurone cells. Bars = 5 μm.

(B) Measurement of diameters of PBIs and PSVs. Values are means ± SD. **P < 0.01 (*n* > 300, *t* test).

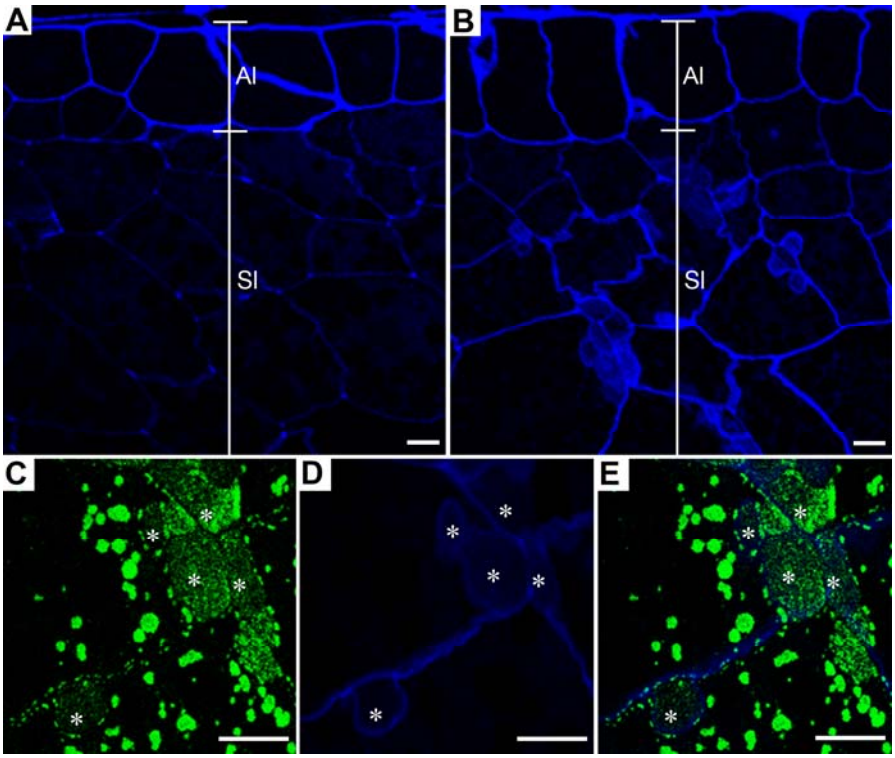

Supplemental Figure 5. Abnormal deposition of cell wall-like materials in the *gpa3* subaleurone cells.

(A) and **(B)** Confocal microscopy images of the cell wall autofluorescence (blue) in wild-type **(A)** and *gpa3* mutant **(B)** grains. Note that the subaleurone cells in the *gpa3* mutant show stronger cell wall autofluorescence signals than the wild-type subaleurone cells. By contrast, the cell wall autofluorescence signals of aleurone layer cell are comparable in the wild type and the *gpa3* mutant. Al, aleurone layer; SI, Subaleurone layers.

(C) to **(E)** High-magnification confocal microscopy images of the PMB structures showing that glutelin-filled PMBs (asterisks) are surrounded by the blue autofluorescence signals, indicating that PMBs may contain cell wall materials. Glutelins were labeled with anti-glutelin acidic subunits antibodies and visualized by secondary antibodies conjugated with Alexa fluor 488 (green). **(E)** Merged image of **(C)** and **(D)**. Bars = 10 μm.

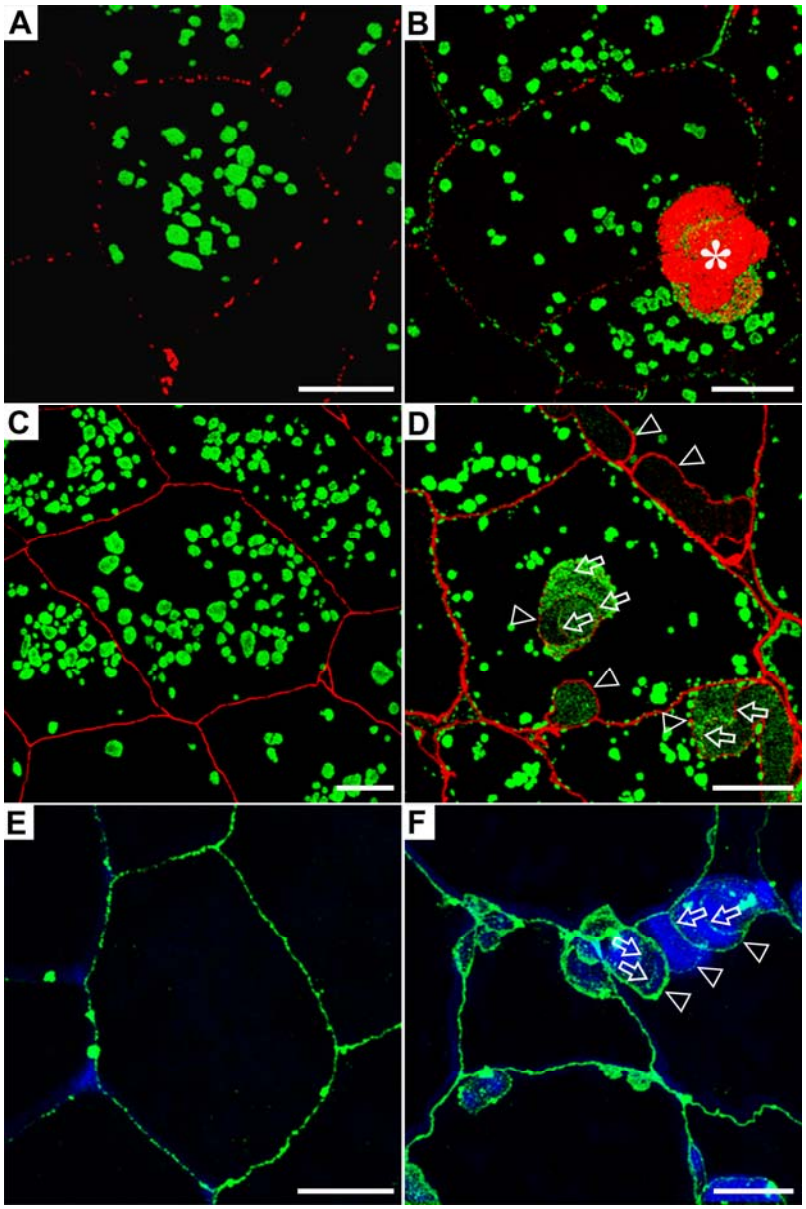

Supplemental Figure 6. Abnormal Accumulation of Cell Wall Components in the PMBs.
(A) and **(B)** Confocal microscopy images showing that callose (red) is localized as dotted structures at the plasmodesmata in both wild-type **(A)** and *gpa3* mutant **(B)** subaleurone cells, but massive callose is abnormally localized inside the PMBs (asterisk) in the *gpa3* mutant **(B)**.
(C) and **(D)** Confocal microscopy images showing stratified appearance of PMBs in *gpa3* mutant. Secondary antibodies conjugated with Alexa fluor 488 (green) and Alexa fluor 555 (red) were used to visualize the glutelins and (1, 3; 1, 4)-β-glucan, respectively.
(E) and **(F)** Confocal images showing that pectin has a similar distribution pattern to (1, 3; 1, 4)-β-glucan in the wild type and *gpa3* mutant. Arrows indicate the pectin inside the PMBs, while arrowheads indicate the pectin outside the PMBs. Pectin was detected using the JIM7 monoclonal antibodies, and visualized with secondary antibodies conjugated with FITC (green), while PMBs were visualized by Calcofluor White (a non-specific dye for β-glucan, blue) staining. Bars = 10 μm.

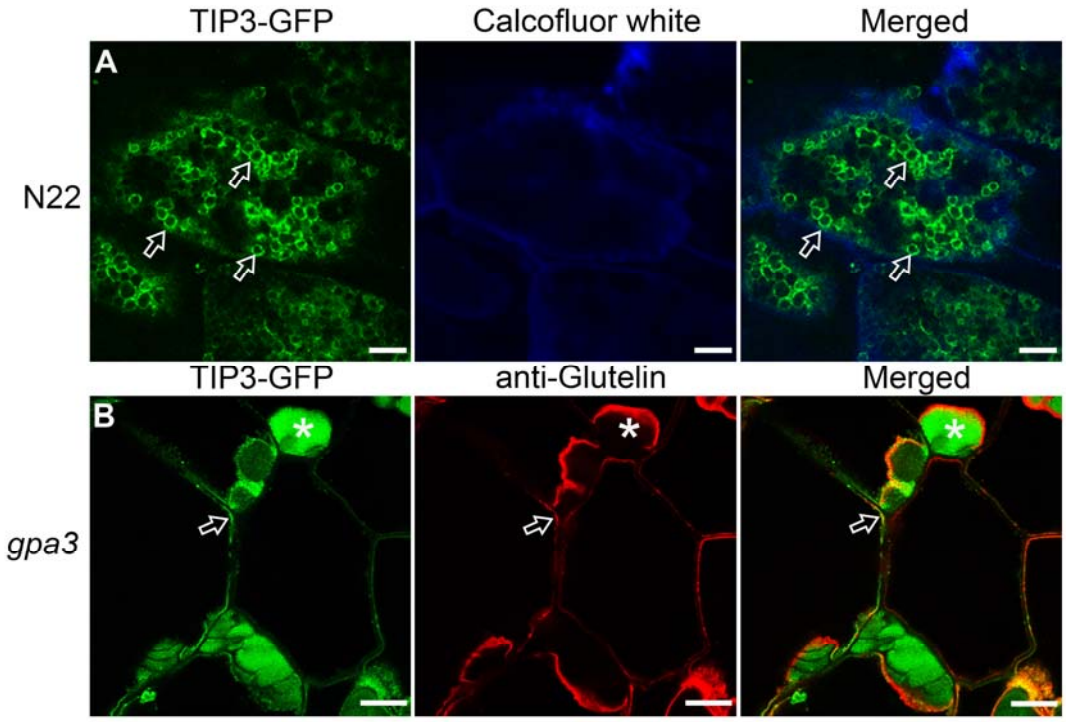

Supplemental Figure 7. Accumulation of TIP3 and glutelins to the apoplast in *gpa3* subaleurone cells.

(A) TIP3-GFP (green) specially distributes to the peripheral regions of PBIIs (arrows) in TIP3-GFP-expressing N22 subaleurone cells (9 DAF). The cell wall was labeled with Calcofluor White (a non-specific dye for β-glucan, blue) staining. N22, a wild-type *indica* var. Bars = 10 μm.

(B) Confocal microscopy images showing that TIP3-GFP (green) is colocalized with glutelins (red) in apoplast (arrow) and PMBs (asterisk) in TIP3-GFP-expressing *gpa3* subaleurone cells (9 DAF). Bars = 10 μm.

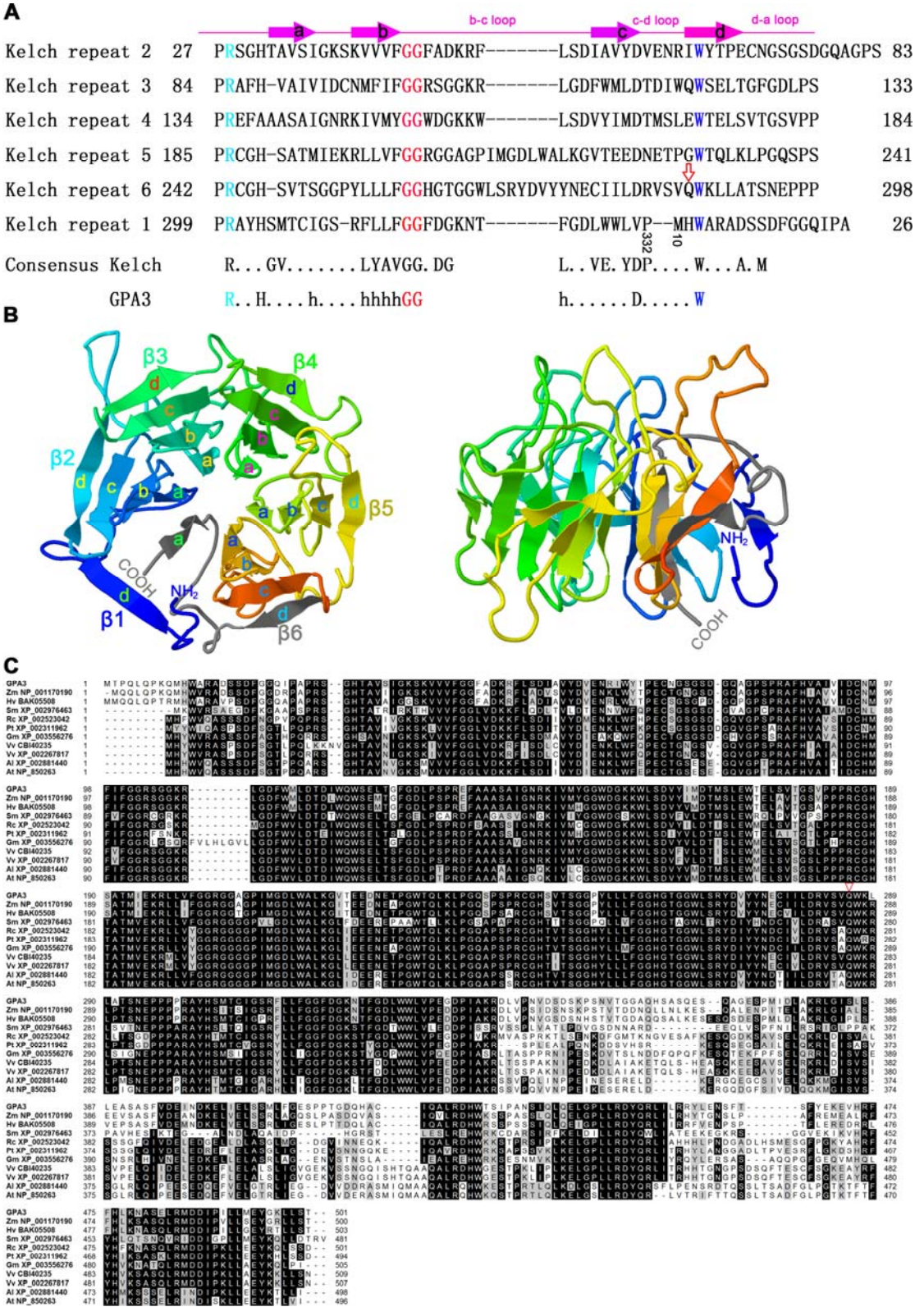

Supplemental Figure 8. Structural and sequence analysis of GPA3.

(A) Amino acid sequence alignment of the six kelch-repeat motifs of GPA3. The general consensus was built according to a previous report (Adams et al., 2000) in which “h” indicates hydrophobic residues. The secondary structure was predicted using The PSIPRED Protein Structure Prediction Server (http://bioinf.cs.ucl.ac.uk/psipred/). The distribution of secondary structure elements is shown above. Identical amino acids are highlighted in colored letters. Red arrow indicates the last amino acid residue of the truncated gpa3 mutant protein.
(B) A three-dimensional model of GPA3 kelch domain. The model was constructed on the basis of its similarity with the kelch domain of human KLHL12 [Protein Data Bank (PDB) 2vpj Chain A] using the SWISS-MODEL program (Bordoli et al., 2009). The model is shown in two orientations: top (left) and side views (right), and is represented as a cartoon. The gray structure indicates the missing part in the truncated gpa3 mutant protein. Due to limited sequence similarity with human KLHL12, the program only selected the N-terminal 310 amino acid residues of GPA3 protein as the aim sequence, although amino acid residues 311-332 were also predicted to form the b- and c-β strands. Therefore, both b- and c-β strands are absent in our predicted model.
(C) Amino acid sequences alignment of rice GPA3 and its homologs in plants. Sequences were aligned using the BioEdit Software using the Clustal W method. Identical and similar amino acids are shaded in black and grey, respectively. Red arrowhead indicates the last amino acid residue in the truncated gpa3 protein sequences. Kelch-repeat proteins from the following organisms were used: Zm, *Zea mays*; Hv, *Hordeum vulgare subsp. Vulgare*; Sm, *Selaginella moellendorffii*; Rc, *Ricinus communis*; Pt, *Populus trichocarpa*; Gm, *Glycine max*; Vv, *Vitis vinifera*; Al, *Arabidopsis lyrata subsp. Lyrata*; At, *Arabidopsis thaliana*. The proteins were named by the abbreviations of the species name with the accession numbers of the corresponding gene in the National Center for Biotechnology Information (NCBI).

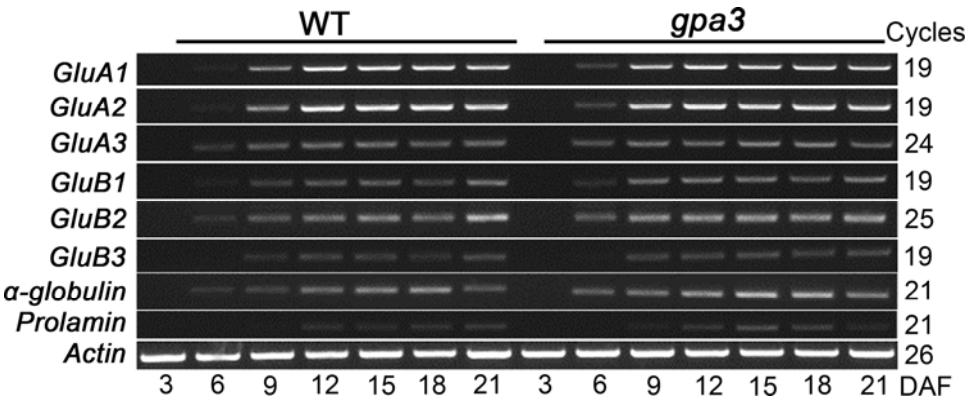

Supplemental Figure 9. Expression analysis of representative storage protein genes at various developmental stages of endosperm.
RT-PCR assay showing that *gpa3* mutation does not obviously affect the expression of several storage protein genes. Actin was used as an internal control. For each RNA sample, three technical replicates were performed. Representative results from two biological replicates are shown. DAF, days after flowering.

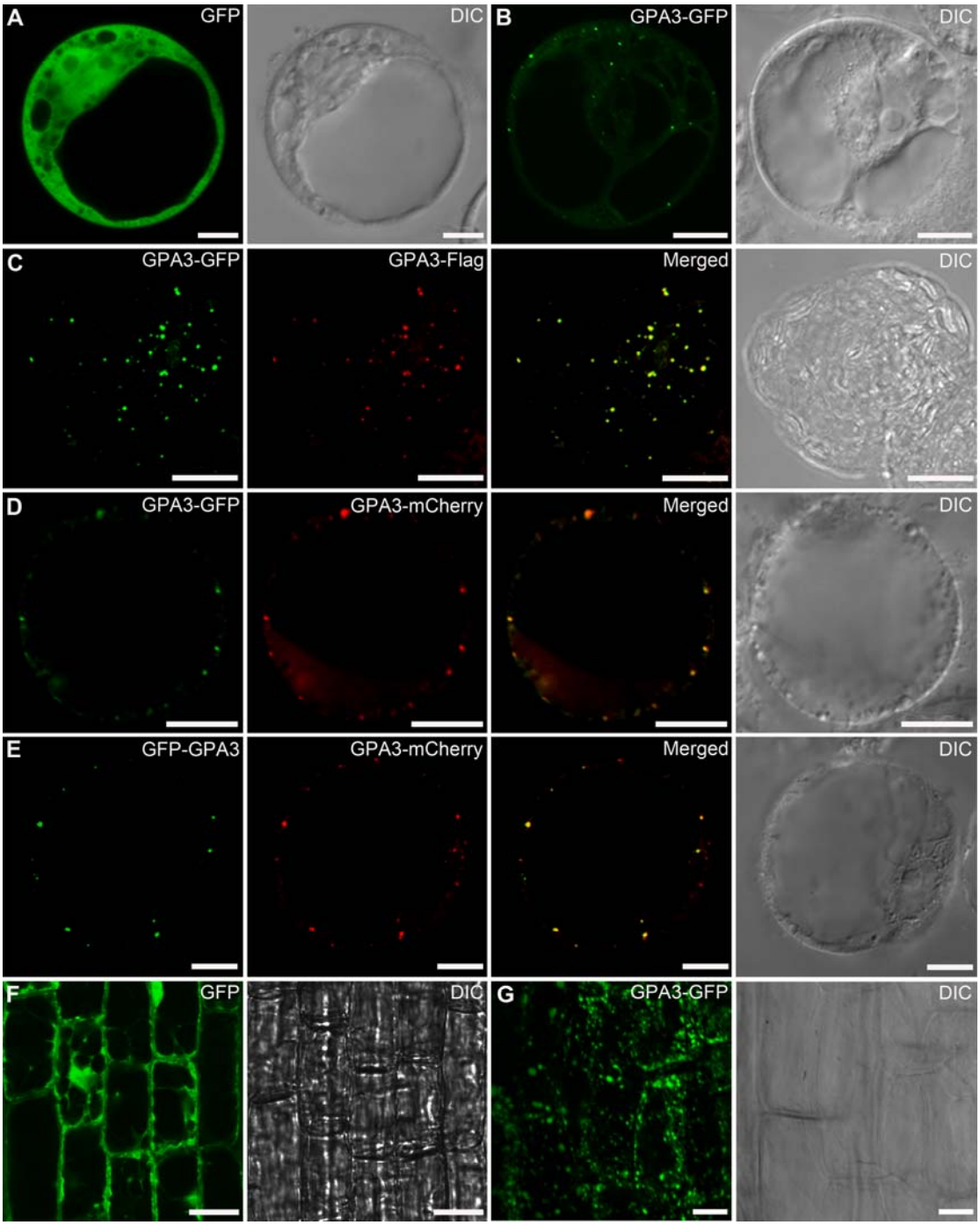

Supplemental Figure 10. Subcellular localization of GPA3 in *Arabidopsis* protoplasts and complemented transgenic rice root cells.

(A) Confocal microscopy images showing that GFP by itself is localized in the cytosol and nucleus in *Arabidopsis* protoplasts. Bars = 10 μm.

(B) Confocal microscopy images showing that GPA3-GFP is localized in punctate structures in *Arabidopsis* protoplasts. Bars = 10 μm.

(C) Confocal microscopy images showing that colocalization of GPA3-GFP (green) and GPA3-Flag (red) in *Arabidopsis* protoplasts. Bars = 10 μm.

(D) Confocal microscopy images showing that colocalization of GPA3-GFP and GPA3-mCherry in *Arabidopsis* protoplasts. Bars = 10 μm.
(E) Confocal microscopy images showing that colocalization of GFP-GPA3 and GPA3-mCherry in *Arabidopsis* protoplasts. Bars = 10 μm.
(F) Confocal microscopy images showing that GFP by itself is localized in the cytosol and nucleus in the root tip cells of transgenic rice plants. Bars = 10 μm.
(G) Confocal microscopy images showing that GPA3-GFP fusion protein is localized to punctate structures in the cytosol in the root cells of complemented transgenic rice plants expressing 35S promoter-driven *GPA3-GFP*. DIC, differential interference contrast. Bars = 10 μm.

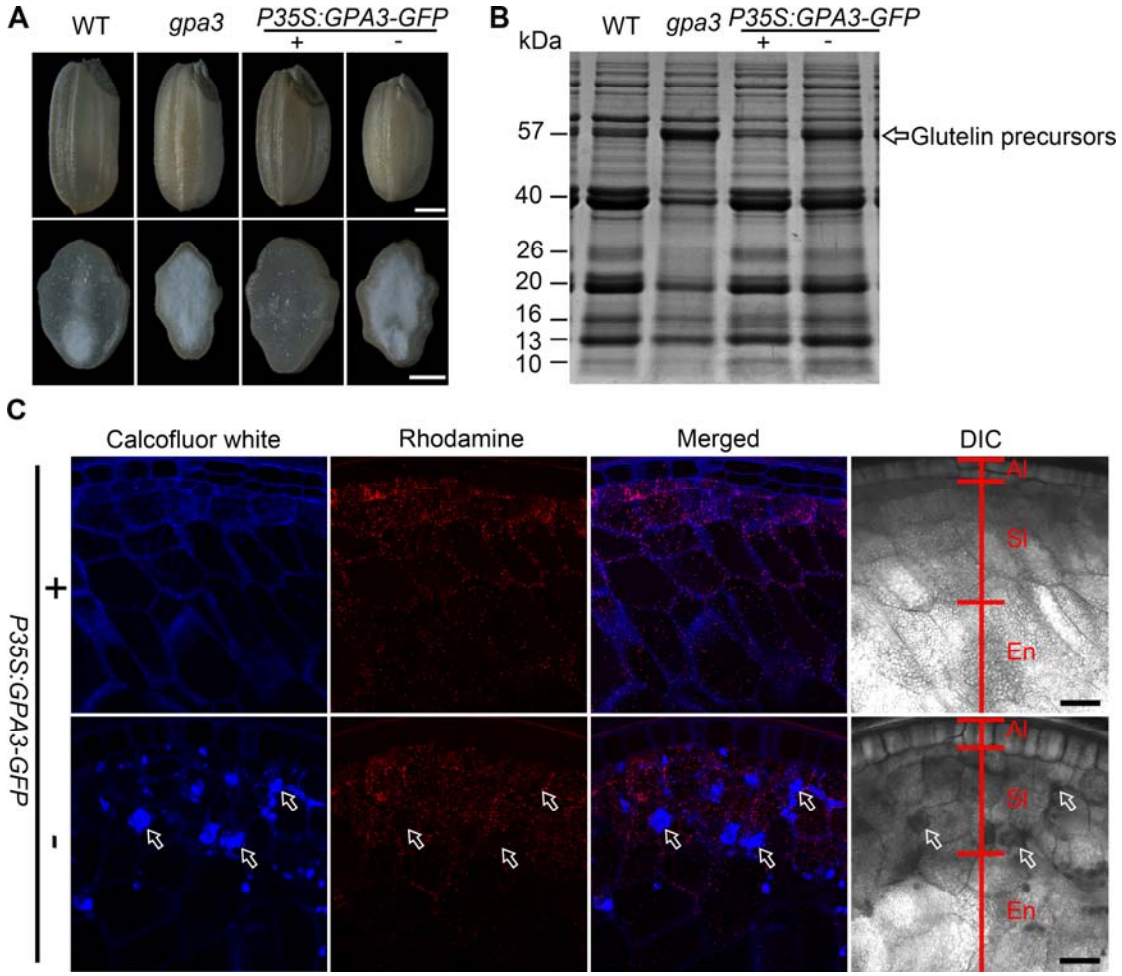

Supplemental Figure 11. Complementation of *gpa3* mutant phenotypes by 35S promoter-driven *GPA3-GFP*.

(A) 35S promoter-driven *GPA3-GFP* transgene rescued the grain phenotype of *gpa3* mutant. Bars = 1 mm.

(B) 35S promoter-driven *GPA3-GFP* transgene rescued the storage protein composition of *gpa3* mutant.

(C) 35S promoter-driven *GPA3-GFP* transgene rescued the storage protein sorting defect of *gpa3* mutant. Rhodamine was used to stain PBIs (red), while calcofluor white was used to stain the cell wall (blue) in wild type, and cell wall as well as cell wall components-containing PMB structures (blue) in *gpa3* mutant. Arrows indicate the PMB structure in *gpa3* mutant. DIC, differential interference contrast. Bars = 50 μm.

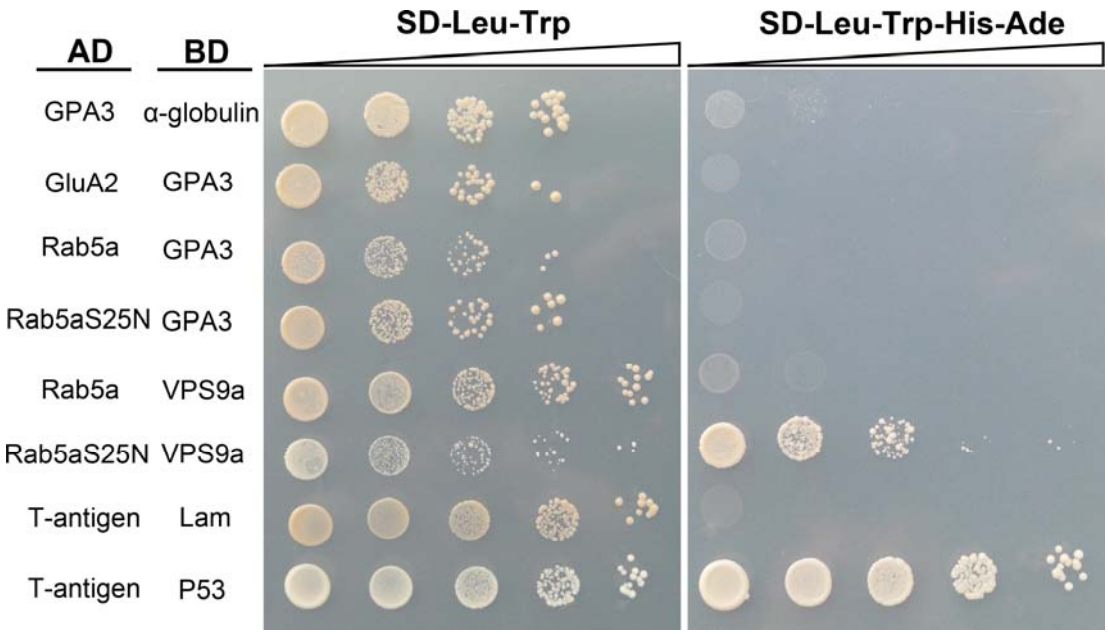

Supplemental Figure 12. Y2H assay between GPA3 and related proteins.
Y2H assay showing that GPA3 does not interact with GluA2, α-globulin, Rab5a, and its GDP-fixed derivative form Rab5aS25N, while VPS9a interacts with Rab5aS25N, but not the wild-type Rab5a.
The interaction between T-antigen and Lam, T-antigen and P53 were used as negative and positive controls, respectively. Cotransformed yeast clones were serial diluted and then placed on SD dropout plates to detect the reporter gene expression.

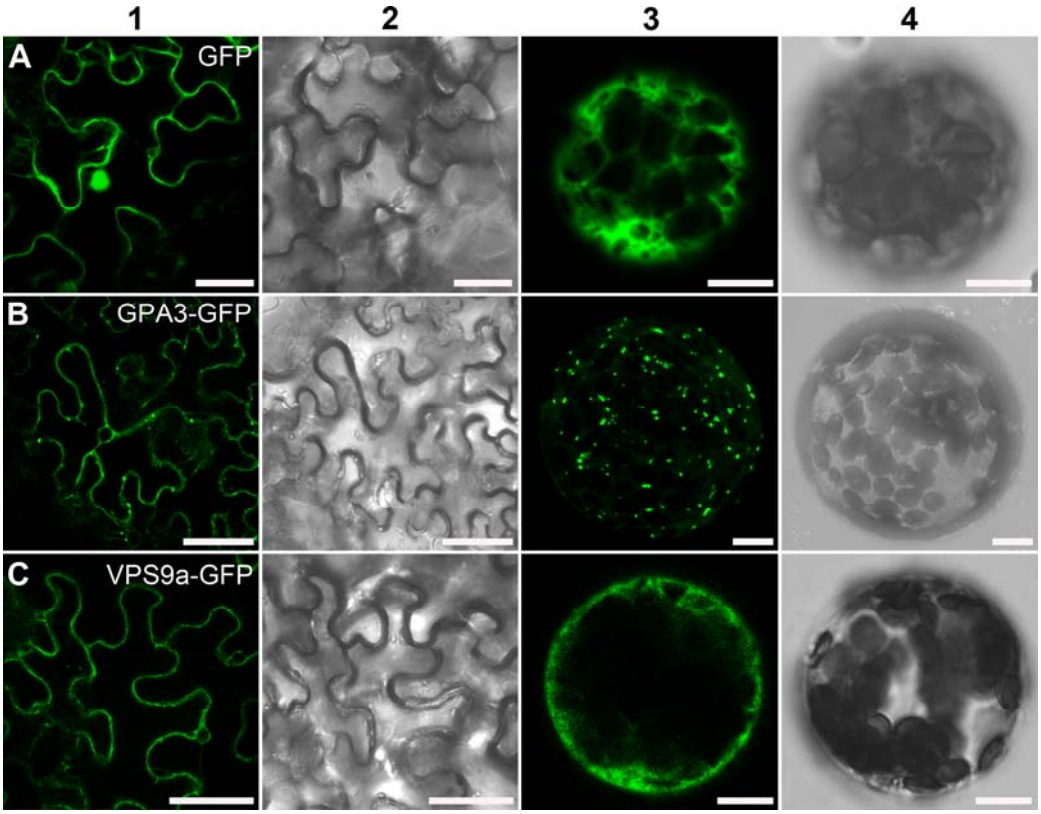

Supplemental Figure 13. Subcellular localization of GPA3 and VPS9a in leaf epidermal cells of *N. benthamiana*.

(A) Confocal microscopy images showing that GFP by itself is localized in the cytosol and nucleus in leaf epidermal cells (column 1 and 2) and protoplasts (column 3 and 4) of *N. benthamiana*.

(B) Confocal microscopy images showing that GPA3-GFP is localized in punctate structures in leaf epidermal cells (column 1 and 2) and protoplasts (column 3 and 4) of *N. benthamiana*.

(C) Confocal microscopy images showing that VPS9a-GFP is localized in the cytosol in leaf epidermal cells (column 1 and 2) and protoplasts (column 3 and 4) of *N. benthamiana*.

Bars in column 1 and 2 = 50 μm; bars in column 3 and 4 = 10 μm.

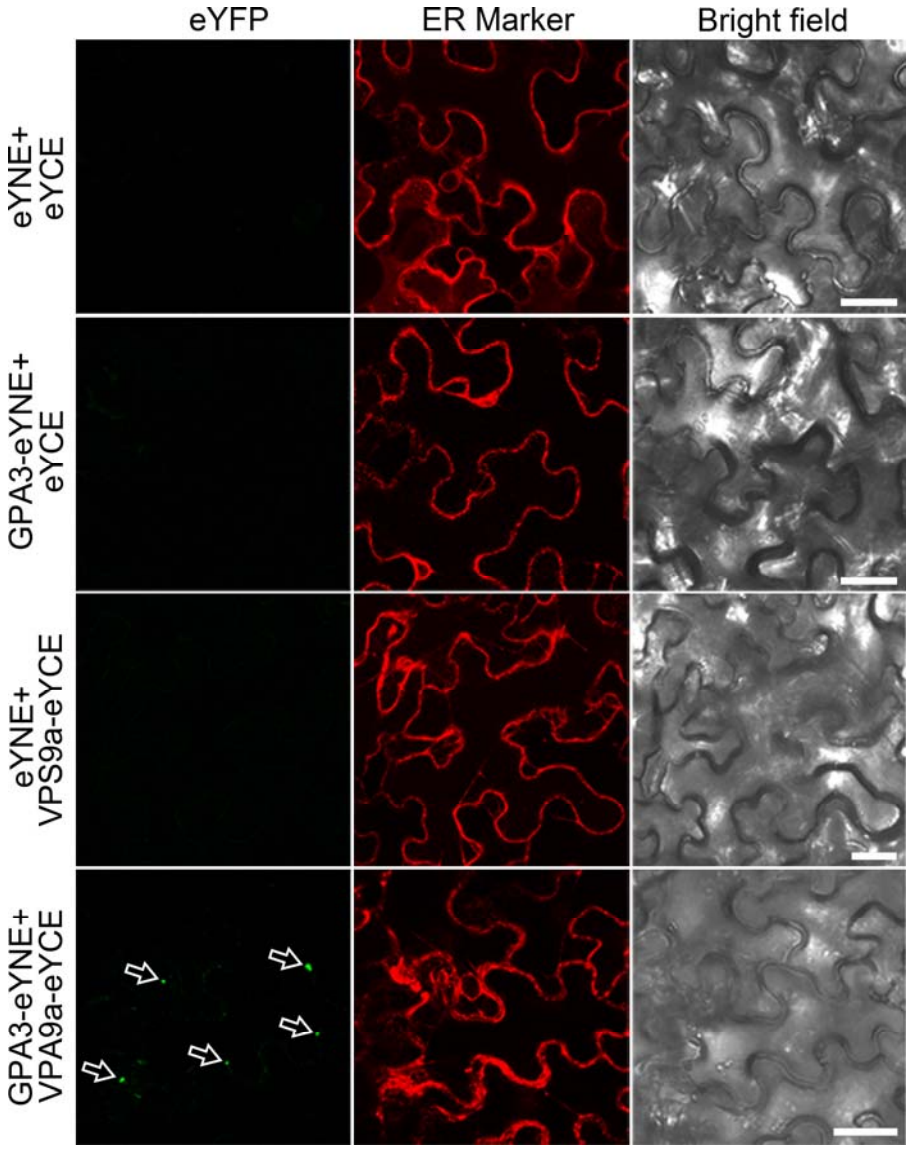

Supplemental Figure 14. BiFC assay of GPA3 and VPS9a in leaf epidermal cells of *N. benthamiana*.
Confocal microscopy images of BiFC assay showing that GPA3 interacts with VPS9a in punctate organelles (green) in leaf epidermal cells of *N. benthamiana*. The signals of eYFP were not detected in the corresponding negative controls. ER marker was used as an expression control (red). Arrows indicate the punctate signals. Bars = 50 μm.

Supplemental Table 1. Characteristics of wild-type and *gpa3* grains.

	Weight (g)[a]	Protein (%)	Amylose (%)	Lipid (%)
Wild type	21.09 ± 0.11	13.27 ± 0.06	22.28 ± 0.45	2.25 ± 0.06
gpa3	14.90 ± 0.05	13.91 ± 0.07	17.44 ± 0.32	4.26 ± 0.14
P value	< 0.01	< 0.05	< 0.01	< 0.01

[a] Weight of 1000 brown grains; Values are means ± SD. (n = 3, t test).

Supplemental Table 2. Segregation of mutant phenotypes in reciprocal crosses between the wild type and the *gpa3* mutant.

Cross	Normal	57H/Floury	$X^2_{3:1}$[a]
gpa3/wild type F_2	125	45	0.1255
wild type/*gpa3* F_2	114	41	0.1053

[a] Value for significance at $P = 0.05$ and 1df is 3.84.

Supplemental Table 3. List of primer pairs used in this study.

Usage	Primer Name	Sequence
Fine mapping	Q6-F	5' TTAGATACGCAAAGACCGAAAGA 3'
	Q6-R	5' GAACACGATACGCTGAAAATGAT 3'
	Q14-F	5' AATGAGATAAAAAAGATA 3'
	Q14-R	5' ACAAGAAGAGGAAAACAG 3'
	Q19-F	5' TTTTAGCCGAATTTGATTCTA 3'
	Q19-R	5' ATTGCTTTATTTTTGGTTGTG 3'
	Q58-F	5' ATTGGCAAGGCGCACAATTC 3'
	Q58-R	5' CATCCTATAACATTTAAAGC 3'
	Q57-F	5' CTATAGTGAAAGGACCGGA 3'
	Q57-R	5' ATGTCCAGACTGCAAAAAGA 3'
	Q49-F	5' GACATCCTTTTTCACACGCG 3'
	Q49-R	5' AAACGAAACGATGACAGTAGC 3'
	Q38-F	5' TTACAGAAAAATTTAACA 3'
	Q38-R	5' ATATTTAATAAAACGAAT 3'
	Q20-F	5' TTGATGGAACTATCTTGG 3'
	Q20-R	5' CTCTCTCGGGTACTCTGC 3'
	Q16-F	5' TCCAAATACACTGTGAAATAG 3'
	Q16-R	5' CAGGAAGAAGAAGATGAAGAA 3'
Genotyping and transgenic identification	Q25-F	5' TCTCTTGTAGCAACCAGCAGTA 3'
	Q25-R	5' AGTCTCGTTTCGCAATAGGAT 3'
	GPA3-dCAPS-F (HinfI)	5' ATTTGGCATCTCAGTCTC**GA**TT 3'
	GPA3-dCAPS-R	5' TCCCCGAATGTATTTTTCC 3'
	Q4041-F	5' GCCAGTTTGTTGAGTTCCAGG 3'
	Q4041-R	5' ACCGCATTTGTGATGTCGTAG 3'
	T5390-F	5' CTCGCTCTACCCTTTACCTACC 3'
	T5390-R	5' GCTTATCCCTTGGAGCCTTAT 3'
	T5390-dCAPS-F (HinfI)	5' ATGATGTTTCACTTTGA**G**ATT 3'
	T5390-dCAPS-R	5' TGGATTGTCTTGTATTGTGATT 3'
	GPA3-CDS-ZJYJC-F	5' GAGTGGCTCGGATGGACAGG 3'
	GPA3-CDS-ZJYJC-R	5' AAAGAAAGTGAAATGCCCAATCG 3'
	GPA3-2F	5' TCAACATTCCGCATCACAGG 3'
	GUS-3R	5' TCGGCTTGTTACGAATGACTTT 3'
Genomic DNA and cDNA cloning	GPA3-Genome-F	5' GTGGGAAGAACTAGGAAGGTTGTCG 3'
	GPA3-Genome-R	5' TGGAAGGAAATAGGGTCACAAGGG 3'
	GPA3-cDNA-F	5' CTACCGTGGAGGCGTGGATTG 3'
	GPA3-cDNA-R	5' CATGCCATGTATGCAGCTATG 3'
	Rab5a-cDNA-F	5' ATCCCTCATCCGATCTGAATC 3'
	Rab5a-cDNA-R	5' GCAGCAGCCACTTTACAAGC 3'
	VPS9a-cDNA-F	5' TACGGCTCCGACAAAATAAAT 3'

	VPS9a-cDNA-R	5' TCTCTGTAACCAGTTGTCACCC 3'
	GluA2-cDNA-F	5' TTCCAATAACATCCTCAAATA 3'
	GluA2-cDNA-R	5' CATAAACTTAGAACAGAACCG 3'
	α-globulin-cDNA-F	5' GATCAGTTCATCACCAACAAACA 3'
	α-globulin-cDNA-R	5' TCCAGAACGCACAAAATCAT 3'
RT-PCR and quantitative RT-PCR	RT-GPA3-F	5' AAGGGCCTTTCACGTAGCT 3'
	RT-GPA3-R	5' TGTCCAACCTGGTGTCTCG 3'
	RT-GluA1-F	5' GGTTGCAAGCATTTGAGCCA 3'
	RT-GluA1-R	5' GGCAACAACTGGCACTTCA 3'
	RT-GluA2-F	5' TGCTTGTTCCTCTTGTGCGA 3'
	RT-GluA2-R	5' TATGGCAACAACCGGCACTT 3'
	RT-GluA3-F	5' TCAATGGCAAAGTTCTCGCC 3'
	RT-GluA3-R	5' AACACCAGCAGGCAATGCAA 3'
	RT-GluB1-F	5' CAGCACAAACCCATGGCATA 3'
	RT-GluB1-R	5' GGTTCAAGCTGATTGGCGTT 3'
	RT-GluB2-F	5' CAAGCACAAACCCATGGCAT 3'
	RT-GluB2-R	5' CAACAACCGATGCATCACCA 3'
	RT-GluB3-F	5' CCGAACGTAAATCCATGGCA 3'
	RT-GluB3-R	5' TGGTGCATCGCCTTCATTGT 3'
	RT-α-Globulin-F	5' GATCAGTTCATCACCAACAAAACA 3'
	RT-α-Globulin-R	5' TCCAGAACGCACAAAATCAT 3'
	RT-Prolamin-F	5' TGAAGCATAGTAGTAGAATCCAACA 3'
	RT-Prolamin-F	5' GACCCTAAGTTTCAACAGTCACA 3'
	RT-Actin-F	5' TGGAACTGGTATGGTCAAGGC 3'
	RT-Actin-R	5' AGTCTCATGGATACCCGCAG 3'
	qRT-GPA3-F	5' GAAGAGGTTGCTTGTATTTGGTG 3'
	qRT-GPA4-R	5' GTGGAGATGGAGATTGTCCTG 3'
	qRT-Tubulin-F	5' GCTCCGTGGCGGTATCAT 3'
	qRT-Tubulin-R	5' CGGCAGTTGACAGCCCTAG 3'
Binary vector construction	GPA3-Infusion-SmaI-F	5' AATTCGAGCTCGGTA**CCCGGG**GTGGGAAGAACTAGGAAGGTTGTCG 3'
	GPA3-Infusion-SmaI-R	5' CGACTCTAGAGGATC**CCCGGG**TGGAAGGAAATAGGGTCACAAGGG 3'
	GPA3-1305-GFP-XbaI-F	5' TAGC**TCTAGA**ATGACGCCGCAGCTGCAGCC 3'
	GPA3-1305-GFP-BamHI-R	5' CCAT**GGATCC**GGTGGAAAGCAGCTTTCCA 3'
	VPS9a-1300-221-Flag-XbaI-F	5' GGAC**TCTAGA**ATGGATGGCGGCGGCGGAGG 3'
	VPS9a-1300-221-Flag-SalI-R	5' CCAT**GTCGAC**TGCATGTTCAGGTTGATCTG 3'
	Rab5a-Myc-Infusion-BamHI-F	5' GAAATCGAT**GGATCC**TAATGGCGGCCAACCCCGGCAA 3'
	Rab5a-Myc-Infusion-BamHI-R	5' CTAGGCTACGTA**GGATCC**TTATGAGCAGCATGAAGAACTG 3'
	GPA3-SPYNE173-XbaI-F	5' GGAC**TCTAGA**ATGACGCCGCAGCTGCAGCC 3'
	GPA3-SPYNE173-SmaI-R	5' **GGG**GGTGGAAAGCAGCTTTCCA 3'
	VPS9a-SPYCE(M)-XbaI-F	5' GGAC**TCTAGA**ATGGATGGCGGCGGCGGAGG 3'
	VPS9a-SPYCE(M)-SmaI-R	5' **GGG**TGCATGTTCAGGTTGATCTG 3'
Prokaryotic expression	GPA3-MBP-BamHI-F	5' ATTC**GGATCC**ATGACGCCGCAGCTGCAGCC 3'

vector construction	GPA3-MBP-SalI-R	5' GCAG**GTCGAC**GGTGGAAAGCAGCTTTCCA 3'
	VPS9a-GST-BamHI-F	5' GCGT**GGATCC**ATGGATGGCGGCGGCGGAGG 3'
	VPS9a-GST-SalI-R	5' TCGA**GTCGAC**CTCATGCATGTTCAGGTTGAT 3'
Yeast two-hybrid vector construction	GPA3-AD-Infusion-EcoRI-F	5' TGGCCATGGAGGCCAGT**GAATTC**ATGACGCCGCAGCTGCAGCC 3'
	GPA3-AD-Infusion-EcoRI-R	5' CGATGCCCACCCGGGTG**GAATTC**TCAGGTGGAAAGCAGCTTTC 3'
	GPA3-BD-Infusion-EcoRI-F	5' ATATGGCCATGGAGGCC**GAATTC**ATGACGCCGCAGCTGCAGCC 3'
	GPA3-BD-Infusion-EcoRI-R	5' GGTCGACGGATCCCCGG**GAATTC**TCAGGTGGAAAGCAGCTTTC 3'
	Rab5a-AD-Infusion-EcoRI-F	5' TGGCCATGGAGGCCAGT**GAATTC**ATGGCGGCCAACCCCGGCAA 3'
	Rab5a-AD-Infusion-EcoRI-R	5' CGATGCCCACCCGGGTG**GAATTC**TTATGAGCAGCATGAAGAACTG 3'
	VPS9a-AD-Infusion-EcoRI-F	5' TGGCCATGGAGGCCAGT**GAATTC**ATGGATGGCGGCGGCGGAGG 3'
	VPS9a-AD-Infusion-EcoRI-R	5' CGATGCCCACCCGGGTG**GAATTC**TCATGCATGTTCAGGTTGAT 3'
	VPS9a-BD-Infusion-EcoRI-F	5' ATATGGCCATGGAGGCC**GAATTC**ATGGATGGCGGCGGCGGAGG 3'
	VPS9a-BD-Infusion-EcoRI-R	5' GGTCGACGGATCCCCGG**GAATTC**TCATGCATGTTCAGGTTGAT 3'
	GluA2-BD-EcoRI-F	5' CAGT**GAATTC**ATGGCATCCATAAATCGCCC 3'
	GluA2-BD-BamHI-R	5' CGAT**GGATCC**CTTAAGAGGATTCCGCCACAT 3'
	α-globulin-BD-Infusion-EcoRI-F	5' CATGGAGGCC**GAATTC**ATGGCTAGCAAGGTCGTCTT 3'
	α-globulin-BD-Infusion-EcoRI-R	5' GGATCCCCGG**GAATTC**CTAGTACTGGCCGGCGGCGA 3'
Transient expression vector construction	GPA3-pAN-XbaI-F	5' TAGC**TCTAGA**ATGACGCCGCAGCTGCAGCC 3'
	GPA3-pAN-BamHI-R	5' CCAT**GGATCC**GGTGGAAAGCAGCTTTCCA 3'
	gpa3-pAN-BamHI-R	5' CCAT**GGATCC**AACAGAGACCCTGTCTAAAA 3'
	GPA3-pAN-NotI-F	5' CCGG**GCGGCCGC**TCAGGTGGAAAGCAGCTTTC 3'
	GPA3-pAN-BglII-R	5' GTAC**AGATCT**ATGACGCCGCAGCTGCAGCC 3'

Supplemental References:

Adams, J., Kelso, R., and Cooley, L. (2000). The kelch repeat superfamily of proteins: propellers of cell function. Trends Cell Biol. **10:** 17-24.

Bordoli, L., Kiefer, F., Arnold, K., Benkert, P., Battey, J., and Schwede, T. (2009). Protein structure homology modeling using SWISS-MODEL workspace. Nat. Protoc. **4:** 1-13.